

Supporting Information for:

Combining Electrocatalysts and Biobased Adsorbents for Sustainable Denitrification

Zili Ma, Matthias Klimpel, Serhiy Budnyk, Anna Rokicińska, Piotr Kuśtrowski, Richard Dronkowski, Aji P. Mathew, Tetyana M. Budnyak,* and Adam Slabon*

Corresponding Authors

Adam Slabon – Department of Materials and Environmental Chemistry, Stockholm University, Svante Arrhenius väg 16 C, 106 91 Stockholm, Sweden; ORCID: 0000-0002-4452-1831; Email: adam.slabon@mmk.su.se

Tetyana M. Budnyak – Department of Materials and Environmental Chemistry, Stockholm University, Svante Arrhenius väg 16 C, 106 91 Stockholm, Sweden; AquaBioSolve Stockholm AB, Svampskogsvägen 16, 1201, 186 55 Vallentuna, Sweden; ORCID: 0000-0003-2112-9308; Email: tetyana.budnyak@mmk.su.se

Authors

Zili Ma – Institute of Inorganic Chemistry, RWTH Aachen University, 52056 Aachen, Germany; ORCID: 0000-0001-7975-9201

Matthias Klimpel – Department of Materials and Environmental Chemistry, Stockholm University, Svante Arrhenius väg 16 C, 106 91 Stockholm, Sweden; ORCID: 0000-0002-2775-2371

Serhiy Budnyk – AC2T research GmbH, Viktor-Kaplan-Str. 2/c, 2700 Wiener Neustadt, Austria ORCID: 0000-0002-2273-0456

Anna Rokicińska – Faculty of Chemistry, Jagiellonian University, Gronostajowa 2, 30-387 Kraków, Poland; ORCID: 0000-0001-8397-4422

Piotr Kuśtrowski – Faculty of Chemistry, Jagiellonian University, Gronostajowa 2, 30-387 Kraków, Poland; ORCID: 0000-0001-8496-0559

Richard Dronkowski – Institute of Inorganic Chemistry, RWTH Aachen University, 52056 Aachen, Germany; Hoffmann Institute of Advanced Materials, Shenzhen Polytechnic, Liuxian Blvd 7098, Shenzhen, 518055, China; ORCID: 0000-0002-1925-9624

Aji P. Mathew – Department of Materials and Environmental Chemistry, Stockholm University, Svante Arrhenius väg 16 C, 106 91 Stockholm, Sweden; ORCID: 0000-0001-8909-3554

Table of Contents:

Figure S1. SEM images of $\text{Cu}_2(\text{OH})_3\text{NO}_3$ NRs. Inset: high magnification image.

Figure S2. Experimental and simulated powder XRD patterns of $\text{Cu}_2(\text{OH})_3\text{NO}_3$ (COD No. 1538408).

Figure S3. SEM images of CuO NRs. Inset: high magnification image.

Figure S4. Experimental and simulated powder XRD patterns of CuO NRs (COD No. 1011148) and Cu NRs (COD No. 4313207).

Figure S5. SEM image of pristine Cu.

Figure S6. Fitting of (a) the Langmuir, (b) Freundlich and (c) Temkin isotherm models of adsorption of ammonium ions onto LS-SiO₂, CF-SiO₂, KL, Biochar and Lewatit at 22 °C, at presence of 0.1M Na₂SO₄ electrolyte (time of contact: 2 h; initial concentration of ammonium ions: 5 – 80 mg·L⁻¹).

Figure S7. TGA curves of thermal decomposition in O₂ atmosphere for LS-SiO₂, CF-SiO₂, initial lignins and silica. (Reprinted from our previous papers Budnyak et al. *ACS Sustainable Chem. Eng.* **2020**, 8, 16262; Budnyak et al. *Nanomaterials* **2018**, 8, 950.)

Figure S8. Influence of phase contact time on ammonium ions adsorption by LS-SiO₂ and KL-SiO₂ (initial concentration of ammonium ions: 5 mg/g, sorbents dosage – 8 g/L, shaking rate – 180 rpm, temperature – 22 °C, time range: 5 – 90 min).

Figure S9. (a) Pseudo-first order plots, (b) pseudo-second order plots and (c) intraparticle diffusion plots for ammonium ions adsorption kinetics by LS-SiO₂ and KL-SiO₂.

Figure S10. Fitting of (a) the Langmuir, (b) Freundlich and (c) Temkin isotherm models of adsorption of ammonium ions under 0.1M Na₂SO₄ or de-ionized H₂O at 22 °C (initial concentration of ammonium ions: 0.5 – 25 mg·L⁻¹, sorbents dosage – 4 g/L, shaking rate – 180 rpm, temperature – 22 °C) with variable phase contact time.

I. Supplemental Figures

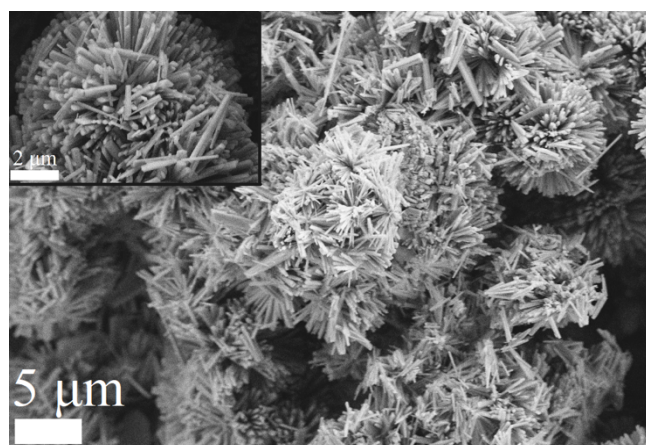


Figure S1. SEM images of Cu₂(OH)₃NO₃ NRs. Inset: high magnification image.

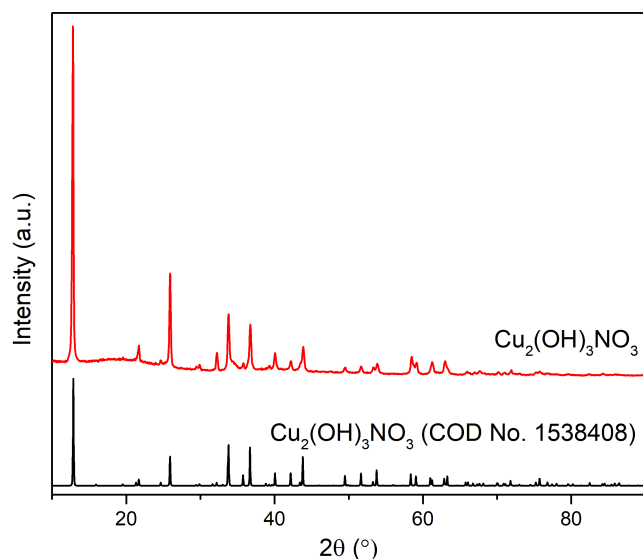


Figure S2. Experimental and simulated powder XRD patterns of Cu₂(OH)₃NO₃ (COD No. 1538408).

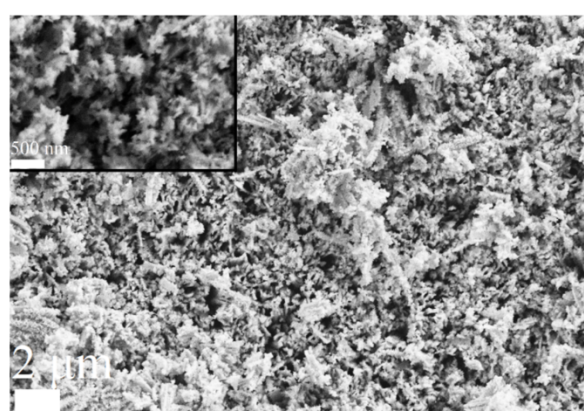


Figure S3. SEM images of CuO NRs. Inset: high magnification image

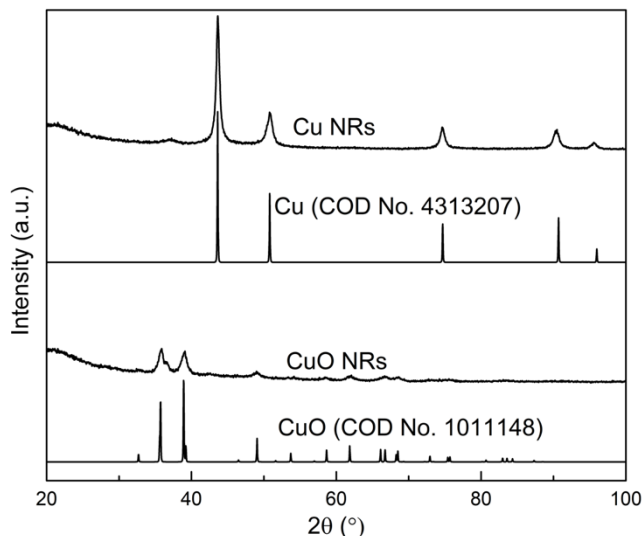


Figure S4. Experimental and simulated powder XRD patterns of CuO NRs (COD No. 1011148) and Cu NRs (COD No. 4313207).

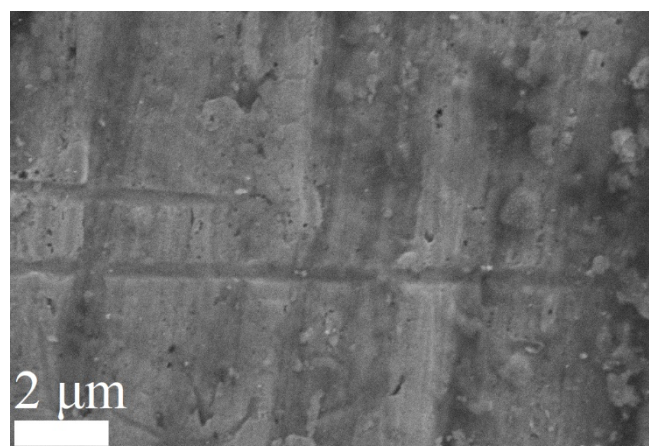


Figure S5. SEM image of pristine Cu.

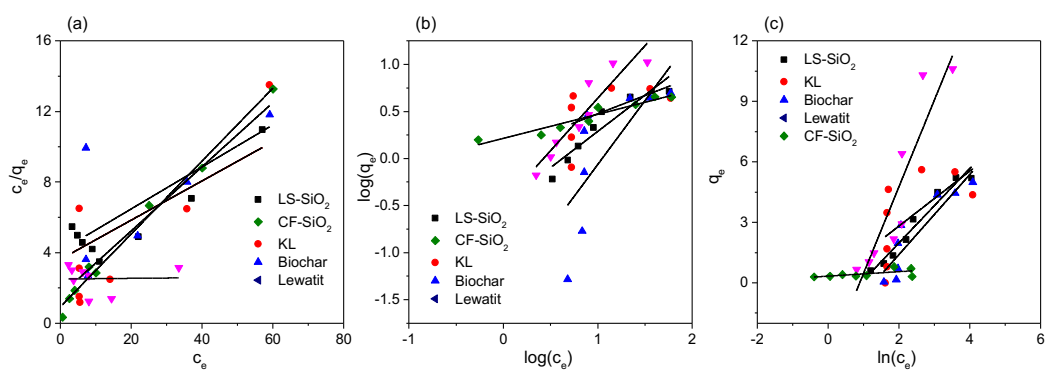


Figure S6. Fitting of (a) the Langmuir, (b) Freundlich and (c) Temkin isotherm models of adsorption of ammonium ions onto LS-SiO₂, CF-SiO₂, KL, Biochar and Lewatit at 22 °C, at presence of 0.1M Na₂SO₄ electrolyte (time of contact: 2 h; initial concentration of ammonium ions: 5 – 80 mg·L⁻¹).

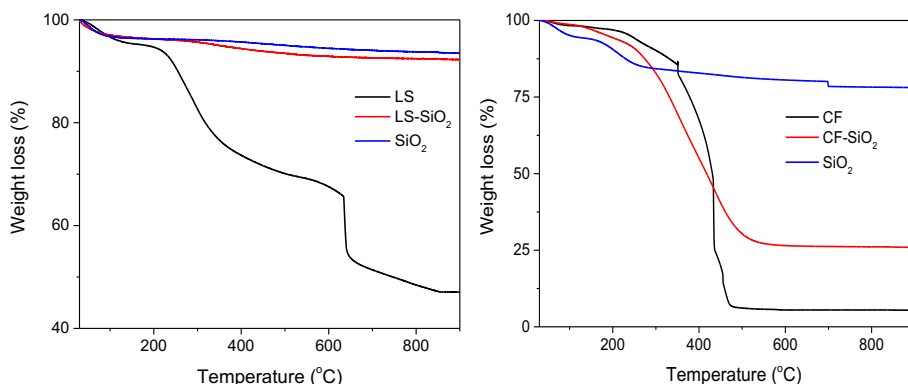


Figure S7. TGA curves of thermal decomposition in O₂ atmosphere for LS-SiO₂, CF-SiO₂, initial lignins and silica. (Reprinted from our previous papers Budnyak et al. *ACS Sustainable Chem. Eng.* **2020**, 8, 16262; Budnyak et al. *Nanomaterials* **2018**, 8, 950.)

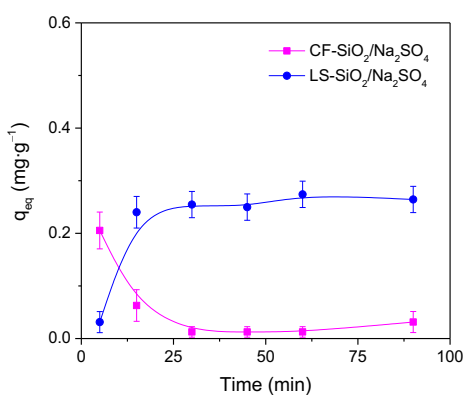


Figure S8. Influence of phase contact time on ammonium ions adsorption by LS-SiO₂ and KL-SiO₂ (initial concentration of ammonium ions: 5 mg/g, sorbents dosage – 8 g/L, shaking rate – 180 rpm, temperature – 22 °C, time range: 5 – 90 min).

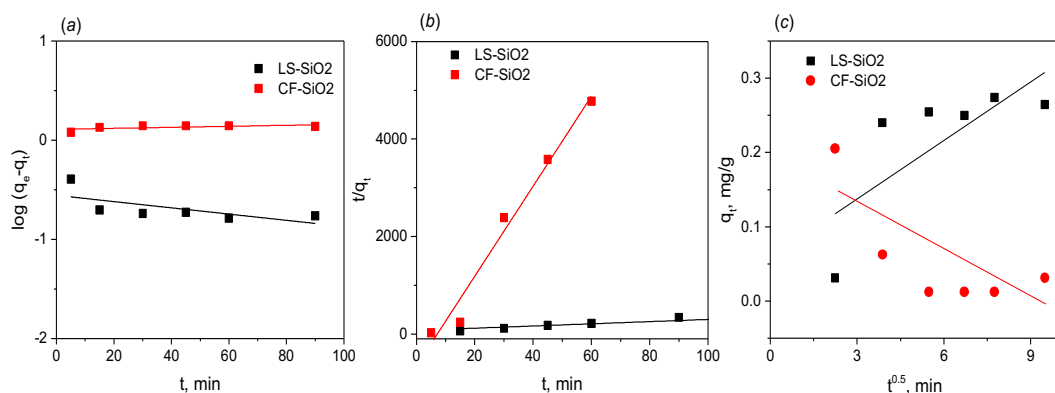


Figure S9. (a) Pseudo-first order plots, (b) pseudo-second order plots and (c) intraparticle diffusion plots for ammonium ions adsorption kinetics by LS-SiO₂ and KL-SiO₂.

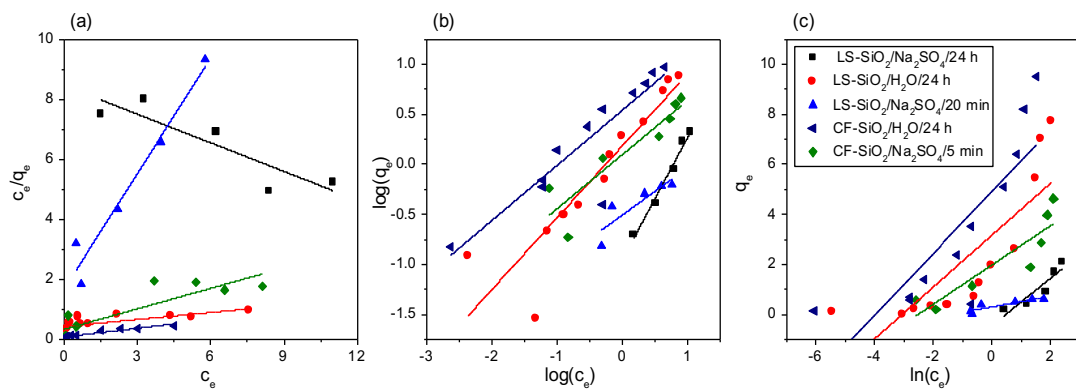


Figure S10. Fitting of (a) the Langmuir, (b) Freundlich and (c) Temkin isotherm models of adsorption of ammonium ions under 0.1M Na₂SO₄ or de-ionized H₂O at 22 °C (initial concentration of ammonium ions: 0.5 – 25 mg·L⁻¹, sorbents dosage – 4 g/L, shaking rate – 180 rpm, temperature – 22 °C) with variable phase contact time.